Available online at www.sciencedirect.com
SCIENCE DIRECT
Science Press
Trans. Nonferrous Met. Soc. China 16(2006) 299−303
Transactions of Nonferrous Metals Society of China
www.csu.edu.cn/ysxb/

Thermal behavior and structure of $Fe_{84}Nb_7B_9$ nanocrystalline powders

CAO Ling-fei(曹玲飞)[1], WANG Ming-pu(汪明朴)[1], XIE Dan(谢 丹)[1],
GUO Ming-xing(郭明星)[1], LI Zhou(李 周)[1], TAN Wang(谭 望)[1, 2], XU Gen-ying(徐根应)[1, 3]

1.School of Materials Science and Engineering, Central South University, Changsha 410083, China;
2. Zhuzhou Cemented Carbide Group Co Ltd, Zhuzhou 412000, China;
3.Department of Science and Technology of Anhui Province,
Hefei 230001, China

Received 9 August 2005; accepted 18 November 2005

Abstract: The thermal behavior of $Fe_{84}Nb_7B_9$ nanocrystalline powders were analyzed by DTA, XRD and TEM measurements. The results show that nanocrystalline powders with grain size of less than 10 nm can be prepared by mechanical alloying. After annealed below 770 ℃, the obtained powders remain in the scale of nanometer without new phases formed, exhibiting good thermal stability. On its DTA curve, a wide temperature interval of 450 ℃ between its two exothermic peaks can be observed. The powders in as-milled state has bcc structure of supersaturated solid solution type, and nanocrystalline together with amorphous phases can be observed in the powder annealed at 350 ℃, which is beneficial for the good soft magnetic properties.

Key words: $Fe_{84}Nb_7B_9$; nanocrystalline; amorphous phases; thermal behavior; magnetic properties

1 Introduction

$Fe_{84}Nb_7B_9$ nanocrystalline alloy is an excellent type of soft magnetic materials, characterized by its high saturation induction, permeability and good noise degeneration property[1, 2]. It can effectively promote the miniature, light, energy-saving and environment-friendly development of electronic devices, and becomes the ideal material for magnetic heads, transformers, inductors and so on. Until now, $Fe_{84}Nb_7B_9$ nanocrystalline alloys prepared by crystallizing amorphous ribbons of rapid solidification have been well investigated[3-8]. The alloy is reported to have a uniform nanostructure mainly consisting of α-Fe grains obtained by crystallizing a fully amorphous phase. Good soft magnetic properties have been achieved for the alloy with the structure consisting of a large portion of nanoscale bcc grains 10-20 nm in size and a small portion of the amorphous phase that likely exists in the grain boundary regions. However, it's difficult to effectively avoid the melting problem caused by the high melting point Nb in rapid solidification. Comparably, mechanical alloying is relatively simple and economical. During this, the alloy with homogenous structure can be obtained by repeating extrusion, deformation, fracture and cold welding of mixed powders under the collision effect among powders, mill balls and vial wall. Though promising in industrial application, to well introduce this technique, relief annealing should be assumed in case the residual stress from milling process deteriorated the soft magnetism of the milled powders. Furthermore, when the powder is manufactured into electronic devices, its thermal stability should be considered in case of the temperature rise during operation. Accordingly, $Fe_{84}Nb_7B_9$ nanocrystalline powders were prepared by mechanical alloying and then their thermal behavior was studied during the subsequent heating process. The emphasis was put on their structure variation during heating, considering that the good soft magnetism of rapidly solidified ribbons mainly results from the composite structure that consists of the nanocrystal phase and intergranular amorphous phase forming in the crystallization (heating) process.

Foundation item: Project(2001BA310A03-1) supported by the National Key Technologies R & D Program of China during the 10th Five-year Plan Period; Project(05JJ30095) supported by the Natural Science Foundation of Hunan Province, China
Corresponding author: CAO Ling-fei; Tel: +86-731-8830264; E-mail: caolingfei@163.com

2 Experimental

Commercial metal powder of Fe, Fe-Nb and B with size of less than 74.6 μm, purity >99%) were blended by its nominal composition Fe-7Nb-9B(mole fraction, %). The mechanical alloying process was performed on a planetary ball mill (QM-1F) at speed of 240 r/min, using stainless steel balls and vials with the mass ratio of ball-to-powder 15∶1 in argon atmosphere. The thermal characterization of powders milled for 96 h was measured by differential thermal analyses(DTA) under flowing argon atmosphere. The subsequent heat treatments were proceeded at 100−850 ℃ for 1 h accordingly. The TEM observation was conducted with a Tecnai G^2 20 transmission electron microscope, and XRD patterns were measured with a DMAX2000(CuK_α) X-ray diffractometer.

3 RESULTS

3.1 Thermal analysis of milled powders

Thermal behavior of $Fe_{84}Nb_7B_9$ powders milled for 96 h was examined by DTA at heating rate of 10 ℃/min. As described in Fig.1, two small exothermic processes between 30−1 200 ℃ appear in the DTA curve, indicating that the powder heated is through two distinct stages. The first exothermic peak has a wide temperature interval of about 450 ℃ between 300-750 ℃, corresponding mainly to the internal strain relaxation of nano-sized bcc phase as confirmed later by X-ray diffractometry. Namely, when heated below 750 ℃, the $Fe_{84}Nb_7B_9$ powder exists with single bcc structure, exhibiting good thermal stability. Meanwhile, during the wide temperature range, only very small variation from the DTA heating baseline can be observed, which suggests that the strain relaxation of bcc phase formed in the mechanical alloying is a long and gentle process. For the second exothermic peak between 770−820 ℃, this corresponds to the formation of new phases (Fe_2B and Fe_3B) , and results in a mixed structure of α-Fe and compounds. To determine an optimal annealing condition to obtain nanocrystalline bcc phase good for the soft magnetism[9, 10], isochronal annealing of the powder can be chosen as follows: 100 ℃ is the typical temperature lower than any exothermic peak, 350, 450 and 770 ℃ correspond to the starting, middle and ending points of the first exothermic process, and 850℃ is higher than the second exothermic temperature.

3.2 XRD evolution during annealing

Structure evolution of $Fe_{84}Nb_7B_9$ powders annealed at different temperatures was determined by X-ray diffractometry. As shown in Fig.2, no new phase can be perceived below annealing temperature of 770 ℃; only at higher temperature, weak peaks of Fe_2B and Fe_3B phases can be observed at 2θ=41° and 46°. Besides the strong peaks that belong to the α-Fe phase, small peaks of $Fe_{0.20}Nb_{0.80}$ at low diffraction angles (about 2θ=35°, 53°) can also be observed without obvious changes. All diffraction peaks before annealing at 770 ℃ are shifted right from its corresponding standard position with better symmetrical shape. According to the Bragg equation $2d\sin\theta=\lambda$, the higher value of diffraction angle θ will result in the smaller interplanar distance d and corresponding smaller lattice constant of bcc structure, as determined from $a=d(H^2+K^2+L^2)^{1/2}$. For example, taking 110 diffraction peak, the main peak of α-Fe phase, into consideration, the lattice constant for as-milled powder is 0.287 08 nm and that for powders annealing at 450 ℃ is 0.286 74 nm. But both lattice constants are larger than the standard value a=0.286 6 nm. Meanwhile, with increasing annealing temperature, the peak breadth of

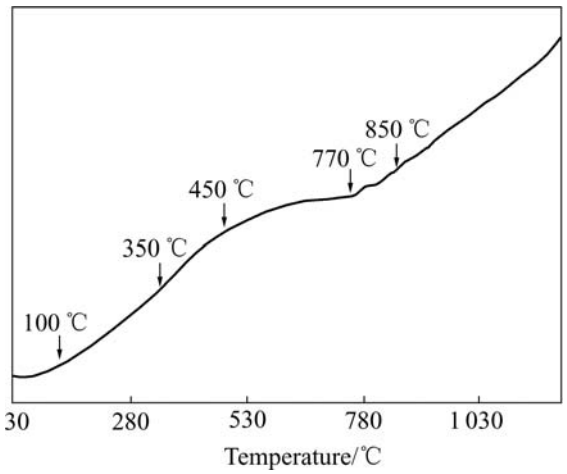

Fig.1 DTA curve of $Fe_{84}Nb_7B_9$ powder after milled for 96 h

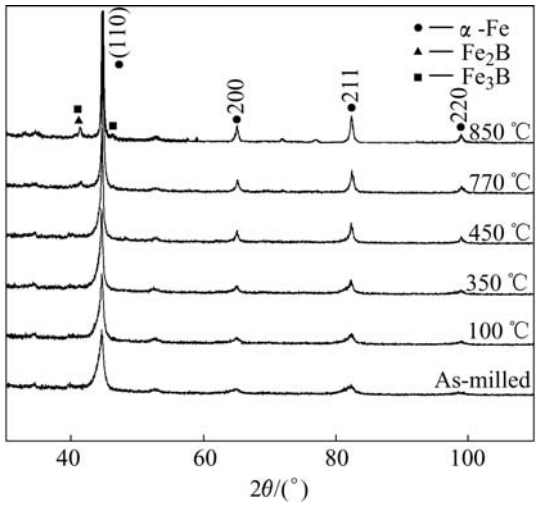

Fig.2 XRD pattern of $Fe_{84}Nb_7B_9$ at different annealing temperatures

XRD profiles tends to a smaller value, and the diffraction peaks of α-Fe phase are gradually sharpened with stronger intensity.

For the peak broadening appearing in XRD patterns, it generally results from five factors as follows: 1) the Cauchy profile broadening caused by small grain size effect; 2) the Gauss profile broadening caused by micro strain inside grains; 3) the intrinsic broadening of diffraction instrument; 4) the overlapping of two sets of diffraction profiles from $K_{\alpha 1}$ and $K_{\alpha 2}$ diffraction of Cu; 5) scattering of background. Among the above five influences, the first two points can provide information of grain size and strain, while the following three points should be eliminated to obtain precise parameters of crystal structures under analysis. To do this, the wave length of Cu $K_{\alpha 1}$ is taken as 0.154 056 nm, $K_{\alpha 2}$ as 0.154 439 nm and the intensify ratio between them is 2∶1. Then $K_{\alpha 2}$ radiation effect can be eliminated by Fourier series separation. The scattering of background can be described by quintic polynomial expression. The third point of diffractometer intrinsic broadening can be handled by using the standard sample Si for contrast. After these, the peak broadening of treated XRD pattern mainly consists of the Cauchy part that caused by grain refinement and Gauss part caused by inner strain effect. Then the XRD profiles can be fitted by Pearson-Ⅶ function[11], $P\,Ⅶ(x)$, which is the combination of Cauchy function and Gauss function with the expression as

$$P\,Ⅶ(x)=I_0\left(1+\frac{x^2}{ma^2}\right)^{-m} \tag{1}$$

$$a=\frac{\beta\Gamma/m}{(m\pi)^{1/2}\,\Gamma\left(m-\frac{1}{2}\right)} \tag{2}$$

where m=1 and $m=\infty$ will represent the Cauchy function and Gauss function, respectively. Based on the Pearson-Ⅶ function, the XRD pattern obtained in experiment can be fitted by the method of least-squares to determine the value of m. Here we get m=1.5. Then the profile shape factor ($2\varpi/\beta$) can be obtained by $2\varpi/\beta=a_0+a_{-1}m^{-1}+a_{-2}m^{-2}$, where a_0=0.934 213, a_{-1}=0.163 317 and a_{-2}=−0.133 719. Then the ratio of integral breadth (β_C^f/β) and (β_G^f/β) can be retrieved in the attached table of the function, and the Cauchy integral breadth β_C^f and Gauss integral breadth β_G^f can be calculated. Finally the average grain size(D) and micro-strain(ε) can be calculated by substituting the fitted integral breadth into

$$D=\frac{K\lambda}{\beta_C^f\cos\theta} \tag{3}$$

and

$$\varepsilon=\frac{1}{4}\beta_G^f\cot\theta \tag{4}$$

where the constants K=0.9 and λ=0.154 05 nm. As described in Fig.3, after milling for 96 h, the α-Fe phase of powders has an average grain size of 8.3 nm and it gradually increases to 10−20 nm during low-temperature annealing. At a higher annealing temperature over 770 ℃, the grain size rises quickly and reaches 57.2 nm at 850 ℃. For the micro-strain, it arrives at its highest before annealing and then falls down before the annealing temperature of 450 ℃. After that, with the formation of Fe_2B and Fe_3B phases, the strain increases obviously along with the increment of annealing temperature.

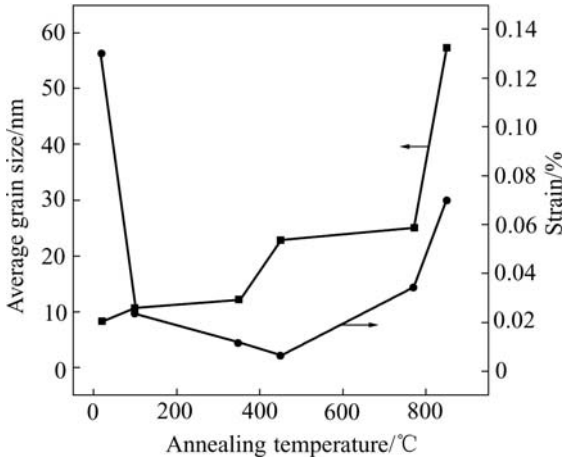

Fig.3 Grain size of $Fe_{84}Nb_7B_9$ at different annealing temperatures

3.3 TEM observation

Powder pattern and structure information can be further determined by transmission electron microscopy. As shown in Fig.4, the milled powders are homogenously distributed with particle diameter about 33 nm. When annealed at 350 ℃, powders tend to aggregate but their component particles can still be discerned to be 20−50 nm in diameter(such areas visible in Fig.4(b) are still composed of several individual grains, namely, the fine particle is a kind of polycrystals as well). It's noted that the selected-area diffraction(SAD) pattern of annealed powders exhibits only the characteristic Debye-Scherrer rings of bcc structure and the miller indices are 110, 200, 211, 220 and 310 respectively. As listed in Table 1, the powder mainly consists of α-Fe nanocrystals with bcc structure, and the measured interplanar distances d are larger than that of its corresponding standard values, which agrees well with the XRD results and suggests that the solution of Nb and B into Fe will enlarge the lattice of α-Fe phase. The above solution effect and structure variation will be discussed later. Meanwhile, it's remarkable that amorphous rings of the SAD on the powder edge can be observed as well,

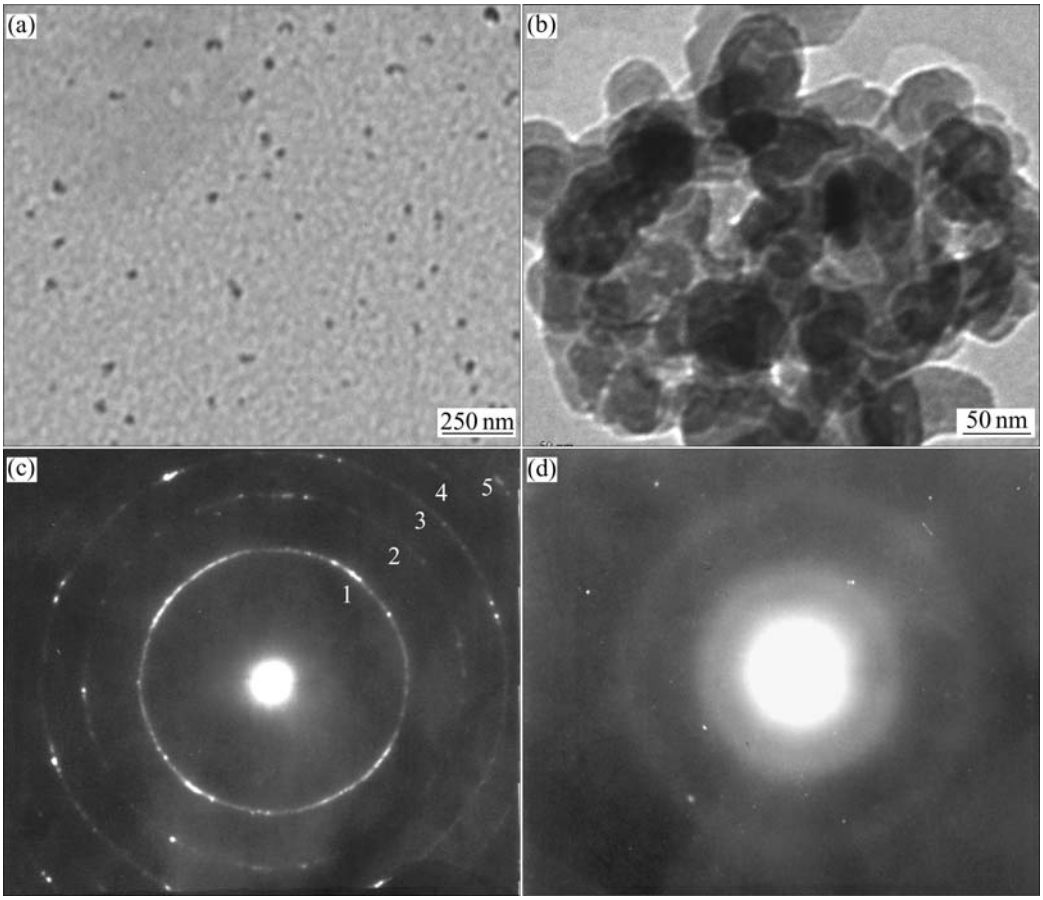

Fig.4 TEM images of $Fe_{84}Nb_7B_9$ powders: (a) As-milled; (b) Annealed at 350 ℃; (c) SAD pattern of (a); (d) SAD pattern of (b)

implying that there exists amorphous structure in the annealing powders. Though there is only quite small amount of amorphous type, which even can not be perceived in the XRD pattern, it may be formed during mechanical alloying, where the intense collision among powder, ball and vial wall will greatly disorder the crystal lattice of powders, and amorphous structure may exist in the powder edges connecting each other[12]. Until now, such nanocrystalline plus amorphous structure appearing together have been only reported in the annealing samples prepared by rapid solidification, and the composite structure has been proved significant to soft magnetic properties in the way that the amorphous phase can benefit the magnetic coupling between nanocrystalline grains[7, 8]. Therefore, it's predicted that our powders obtained by mechanical alloying may exhibit good soft magnetism as well.

Table 1 Index of polycrystallines rings in Fig.4(c)

No.	d/nm	$d_{\alpha\text{-Fe}}$/nm	hkl
1	0.203 5	0.202 7	110
2	0.143 4	0.143 3	200
3	0.118 1	0.117 0	211
4	0.102 1	0.101 3	220
5	0.090 7	0.090 6	310

4 Discussion

Remarkable points of the thermal behaviour of $Fe_{84}Nb_7B_9$ nanocrystalline powders can be figured out by combining DTA, XRD and TEM analysis. The powder exhibits good thermal stability, for its exothermic peak on DTA curve between 300-750 ℃ does not correspond to the formation of new crystal phases, instead it relates the relaxation of inter strain. Then the powder may be effectively softened for the subsequent sintering or other forming technology, which will be verified in another paper. Also, the small value of peak area within a wide temperature interval implies that the exothermic process is slow and gentle.

Thus the powder as magnetic materials can be applied in a wide temperature range, or else if the powder is used as the precursor for bulks, the consolidation process can be proceeded below 750 ℃ to remain the single bcc phase with average grain size below 25 nm. In our experiment, the $Fe_{84}Nb_7B_9$ nanocrystalline bulk has been obtained with homogenous and dense structure, and its average grain size has been determined by XRD analysis to be 22.7 nm, which is important to its magnetic properties and application. When the grain size decreases below the ferromagnetic

exchange length, the magnetization is no longer constrained to follow the easy directions of each individual grain, then the effective average magnetic anisotropy is greatly reduced, permeability and saturation magnetization are enhanced accordingly. Good soft magnetic properties have been achieved for the $Fe_{84}Nb_7B_9$ alloy[3, 7, 9] with the structure consisting of a large portion of nanoscale bcc grains 10−20 nm in size and a small portion of the amorphous phase in the grain boundary regions. Similarly typical structure has been found in our annealed powders by TEM observation as well, suggesting that annealing the mechanical alloyed powders will exhibit the potential of good magnetic properties.

For the basic bcc structure in the milled and annealed powders, it can be further determined as the supersaturated solid solution type. Judging from the XRD pattern of the milled $Fe_{84}Nb_7B_9$ powder, no diffraction peaks of Nb and B can be observed, namely, Nb and B have been milled and solved into the lattice of α-Fe phase. Generally speaking, the solid solution type that two different atoms will constitute should strongly depend on their atom radius[13]. The substitution type is hard to be formed with the radius ratio Δr beyond 30%, where $\Delta r=(r_A-r_B)/r_A$, r_A and r_B are the radius of solvent atom and solute atom, respectively. Taking the $Fe_{84}Nb_7B_9$ alloy into consideration, the empirical radius values[14] of Fe, Nb and B are 0.140 nm, 0. 142 9 nm and 0.085 nm, respectively. Regarding the α-Fe as the solvent, the value of Δr between Fe and B is 39%，Fe and Nb is 2.9%. Then it's deduced that Nb is solved in Fe to form the substitution solid solution, while B and Fe combine the interstitial type. Moreover, the weight proportion of Nb and Fe in the nominal composition of $Fe_{84}Nb_7B_9$ is 13.92%, far beyond the solid solubility limit marked on the phase diagram (<5%). Accordingly the solid solution between Fe and Nb is a supersaturated type and so is to Fe and B.

Above all, much attention should also be paid to the structure uniformity and grain size distribution. In the production of nanocrystalline bcc FeNbB bulk alloys by warm extrusion, KOJIMA et al[15] pointed out that the inhomogeneous grain growth of the bcc phase during annealing would lead to the formation of an inhomogeneous microstructure and result in the larger coercive force Hc value. Recently, based on the random anisotropy model(RAM), MAKINO et al[10] suggested that the effective magnetic anisotropy increased with increasing width of the grain-size distribution even if the mean grain size was constant, and the inhomogeneity of the grain size would increase the coercive force. Accordingly, in the mechanical alloying, powders should be milled long enough to be homogenized. As seen from Fig.4(a), the $Fe_{84}Nb_7B_9$ powder milled for 96 h can satisfy this requirement.

5 Conclusions

1) $Fe_{84}Nb_7B_9$ powders prepared by mechanical alloying for 96 h have the average grain size less than 10 nm. When annealed at 100−850 ℃, the grain size remains in the scale of nanometer.

2) No new phases form when the powder annealing below 770 ℃, the powder exhibiting good thermal stability.

3) The powders in as-milled state has the bcc structure of supersaturated solid solution type, and nanocrystalline together with amorphous phases can be observed in the powder annealing at 350 ℃, which is beneficial for the good soft magnetic properties.

References

[1] MAKINO A，BITOHA T, INOUE A．Nb-poor Fe-Nb-B nanocrystalline soft magnetic alloys with small amount of P and Cu prepared by melt-spinning in air[J]．Scripta Mater, 2003, 48: 869−874.

[2] MAKINO A，INOUE A，MASUMOTO T. Nanocrystalline soft magnetic Fe-M-B(M=Zr, Hf, Nb), Fe-M-O(M=Zr, Hf, Rare earth) alloys and their applications[J]. Nanostructured Materials，1999, 12: 825−828.

[3] MAKINO A，YAMAMOTO Y，HIROTSU Y. Microstucture of nanocrystalline b.c.c. Fe-M-B(M≡Nb, Hf) soft magnetic alloys[J]. Mater Sci and Engi，1994，A179/A180: 495−500.

[4] ZHI Qi-zheng, WANG Ji-jie, CHEN Wen-zhi, HE Kai-yuan. Structure and magnetic properties of nanocrystalline Fe-Nb-B alloys[J]. Journal of Northeastern University (Natural Science), 2004, 25(11): 1072−1075.(in Chinese)

[5] ŠKORVÁNEK I，DUHAJ P， GRÖSSINGER R. Low-temperature magnetic behaviour in amorphous and nanmcrystalline Fe-Nb-B alloys[J]. J of Magn and Magn Mater，2000, 215−216: 431−433.

[6] IMAFUKU M, SATO S, KOSHIBA H. Structural variation of Fe-Nb-B metallic glasses during crystallization process[J]. Scripta Mater, 2001, 44: 2369−2372.

[7] MAKINO A，INOUE A，MASUMOTO T. Nanocrystalline soft magnetic Fe-M-B (M=Zr, Hf, Nb) alloys produced by crystallization of amorphous phase[J]. Mater Trans JIM, 1995, 36(7): 924−938.

[8] GAO You-hui, SHINDO D. Mediated exchange interaction in Fe-Nb-B nanocrystalline soft magnetic materials [J]. Physical Review B, 2003, 67: 172409−4.

[9] HERZER G. Magnetization process in nanocrystalline ferromagnets[J]. Mater Sci and Engi, 1991, A133: 1−5.

[10] BITOHA T, MAKINO A，INOUE A. The effect of grain-size distribution on coercivity in nanocrystalline soft magnetic alloys[J]. J of Magn and Magn Mater, 2004, 272−276: 1445−1446.

[11] GUI Li-feng, TANG Ru-jun. Testing Manual of Mechanical Engineering Materials[M]. Liaoning: Science and Technology Press, 1999. 433−441.(in Chinese)

[12] JU Yi, LI Zong-quan. The mechanisms of mechanical alloying and the application in the field of magnetic materials[J]. Functional Materials, 2002, 33(1): 12−14.(in Chinese)

[13] HOU Zeng-shou, LU Guang-xi. The Principle of Metal Science[M]. Shanghai: Science and Technology Press, 1993. 50−59.(in Chinese)

[14] Mark Winter. Webelements[M]. UK: The University of Sheffield and Webelements Ltd, 2005.

[15] KOJIMA A，HIDEHIKO H，MAKINO A. Soft-magnetic properties of nanocrystalline bcc Fe-(Nb, Zr)-B bulk alloys consolidated by warm extrusion[J]. Mater Trans, JIM, 1995, 36(7): 945−951.

(Edited by LONG Huai-zhong)